Revista Mexicana de Astronomía y Astrofísica, **50**, 87–92 (2014)

INVESTIGATION OF THE 0.84-M TELESCOPE GUIDING AT THE OAN-SPM

V. G. Orlov,[1] D. Hiriart, [2] and V. V. Voitsekhovich[1]

Received 2013 June 24; accepted 2013 December 17

RESUMEN

Reportamos los resultados de una investigación experimental sobre el guiado del telescopio de 0.84-m en el Observatorio Nacional Sierra de San Pedro Mártir, Mxico. Se realizaron observaciones con una cámara EMCCD Andor Luca-S, que permite registrar conjuntos de imágenes de corta exposición. El análisis de los datos muestra que existen tres tipos de errores en el guiado: una tendencia lineal, vibraciones del telescopio, y brincos abruptos.

ABSTRACT

We report the results of experimental investigations of the 0.84-m telescope guiding at the Observatorio Astronómico Nacional at Sierra San Pedro Mártir, Mexico. The observations were carried out with an EMCCD Andor Luca-S camera which allows one to record sets of short-exposure images. The analysis of the data shows that three types of telescope guiding errors are present: linear trend, telescope vibrations, and telescope jumps.

Key Words: instrumentation: high angular resolution — techniques: image processing — telescopes

1. INTRODUCTION

The 0.84-m telescope of the Observatorio Astronomico Nacional (OAN) is located at the astronomical site of Sierra San Pedro Mártir, Mexico. This relatively small telescope is mainly used for photometric observations because more than 60% of the nights at this site have photometric quality (Tapia 2003). However, in order to achieve a good quality of photometric data and imaging, the systematic instabilities of the point spread function (PSF) must be minimized.

There are three main factors which affect the shape of PSF: atmospheric distortions, telescope aberrations and the telescope guiding. It is known that the seeing at San Pedro Mártir is under 1 arcsec throughout one night (Schöck et al. 2009; Michel et al. 2003; Echevarría et al. 1998) and the telescope aberrations are of the same magnitude. However because the quality of the telescope guiding system has newer been investigated, we decided to perform this study.

The 0.84-m telescope is a Ritchey-Chrétien, f/15 telescope with 16 arcsec/mm pixel scale at the focal plane. The telescope has an equatorial yoke mount. Diurnal motion of the telescope is provided by a helical worm gear pair driven by a single dc-motor with a computer-controlled optical encoder.

Since 1996 the 0.84-m telescope is equipped with an off-axis guider (Valdez et al. 1997; Zazueta 1995) which was designed to keep the stellar image inside a certain area on the detector during long-exposure observations. In general, the off-axis guider works well, but sometimes unexpected image distortions along the tracking direction appear.

There are three main types of telescope guiding errors: linear trend, telescope vibrations, and telescope jumps (Voitsekhovich et al. 2007). The analysis of the data obtained has shown that all of them are present. Contrary to the case of short-exposure images where telescope motions can be neglected (Altarac et al. 2001), in our case they appear to be a main reason for the distortion of the shape of the long-exposure PSF.

2. OBSERVATIONS

Observations were made during the nights of May 26 and 27, 2013. The weather conditions were not

[1]Instituto de Astronomía, Universidad Nacional Autónoma de México, México, D.F., Mexico.

[2]Instituto de Astronomía, Universidad Nacional Autónoma de México, Ensenada, B.C., Mexico.

very good, the wind speed was in the range of 2–12 km/h, but at the end of the first night the wind gusts reached up to 30 km/h. In total, we observed 17 bright stars with $m_V \sim 4-8$ mag at different telescope positions with declinations ranging from −31 to 69 degrees.

The observations were carried out using the EM CCD *Luca-S* camera from Andor Technology[3]. Despite its relatively low price this camera has a good quality and is frequently used in astronomical observations (Tokovinin & Cantarutti 2008). The camera provides a simple signal interface via USB port and the quantum efficiency of its detector is higher than 40% in the range of 400 to 680 nanometers. Also, because the camera allows a fast frame grabbing, it can be used for high resolution imaging (Tokovinin & Cantarutti 2008). Because the main interest of our observations is concentrated on image distortions caused by telescope movements which are relatively slow compared to atmospherically-induced ones, all our data were grabbed with a speed equal to 10 frames per second.

During the observations we used only one narrow-band filter 6650/80 nm for all the objects. This filter allows one to minimize the influence of the atmospheric dispersion for large zenith distances. Each data set consists of 3000 short-exposure (100 ms) frames 300×200 px, with a scaling equal to 0.062 arcsec/pixel. For each star, we obtained three sets of data which were taken under the following conditions: the off-axis guider was switched off, the off-axis guider was switched on, and the sky image was captured near to the star. The last kind of sets is necessary because the observations were performed during the full moon phase.

3. DATA PROCESSING

A common method for studying the quality of a telescope guiding system is to analyze the motion of a star image centroid (Voitsekhovich et al. 2007). Let us assume that we have a set of short-exposure images $I(x, y, t)$, where (x, y) are pixels coordinates, or spatial coordinates, and t denotes the number of the image in the set, or a temporal coordinate. The first step of data processing is the sky brightness correction. We simply subtracted an averaged sky image captured near to the star from each short-exposure image. The second step is the calculation of the centroid for each star image. The time-dependent star image centroids $x_c(t)$ and $y_c(t)$ are calculated by the following formulas:

$$\begin{aligned} x_c(t) &= \sum_{xy} xI(x,y,t) \,/\, \sum_{xy} I(x,y,t), \\ y_c(t) &= \sum_{xy} yI(x,y,t) \,/\, \sum_{xy} I(x,y,t), \end{aligned} \tag{1}$$

where the summation is over all the pixels x and y that have the stellar image in the sub-frame .

For simplicity of the data processing, the camera was oriented in such a way that the X-axis was directed along the right ascension. Thus, the Y-axis was oriented along the declination. Figure 1 shows an example of the temporal dependency of a star image centroid along the X-axis (guiding direction) and the Y-axis (declination direction).

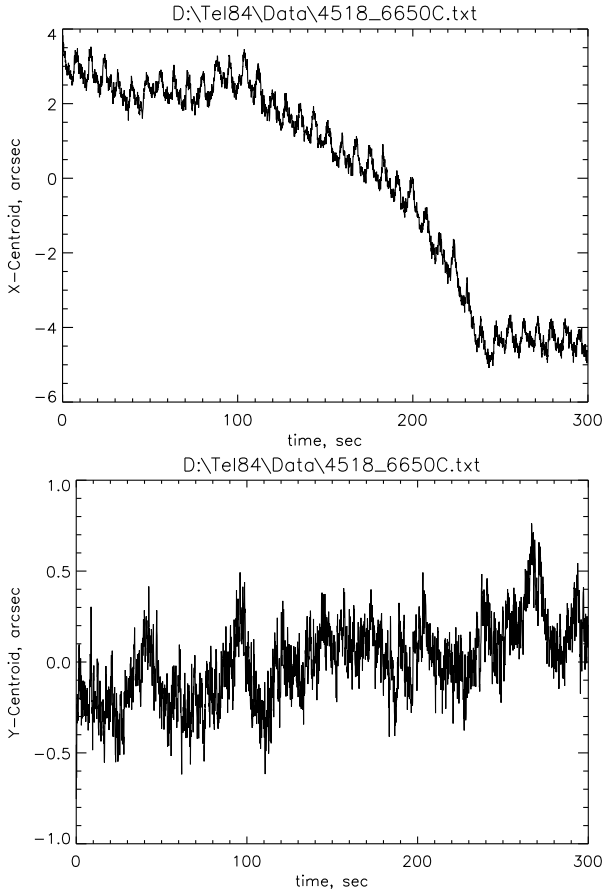

Fig. 1. An example of the temporal displacement of the star image centroid along the X-axis (upper panel) and the Y-axis (bottom panel). Guiding direction is along the X-axis. In both cases, it can be noticed a high frequency component overlaying a long term trend. A small and nearly monotonic drifting may be seen in the Y-direction that might reflect the non-orthogonality between the RA and Dec. axis of the telescope.

[3]Website for Andor Technology: `www.andor.com`.

4. QUALITATIVE ANALYSIS

Analysing the data we found that three main types of telescope guiding errors are present: a linear trend, telescope vibrations, and telescope jumps. In this section a qualitative assessment of the telescope performance is presented, describing some examples for each case of guiding errors.

4.1. *Telescope long-term linear trend*

When the telescope off-axis guider is on, we found that the main telescope linear trend appears in the guiding X-direction: all images are moving along the east-west direction. The speed of this trend is not a constant and it is not permanent (see Figure 1). The long-term trend taking place along the Y-direction (declination) is nearly monotonic, it is much slower and smaller than that one along the X-direction. The drifting along the Y-direction might reflect a small error in the orthogonality between the RA and declination axes of the telescope. There are short-exposure frames where the speed of the trend is nearly zero. However, there are also frames where a high speed linear trend is taking place. This trend can be seen more clearly when the off-axis guider is switched off.

Figure 2 shows an example of the displacement of the centroid cleaned from high-frequency oscillations when the off-axis guider is on. To clean the high frequency oscillations, we used a standard Fourier filter with the following apodization function $w(n)$:

$$w(n) = \begin{cases} 1, \text{ when } 0 \le n \le N_c/2 \\ 0.5{+}0.5\cos\left(\pi \frac{n}{N_c}\right) \text{ when } N_c/2{<}n{\le}N_c \\ 0, \text{ when } n{>}N_c \end{cases}, \quad (2)$$

where N_c is the cut-off frequency that we choose as $N_c = 0.1$ Hz.

Figure 2 shows how the image centroid is shifted by about 6 arcsec during 100 seconds. After that, the centroid does not move at all during the next 100 seconds. Then it starts to move again in the same direction, i.e. from east to west.

The velocity of the centroid movement coincides with the angular velocity of the star across the sky. Analyzing the graph one can conclude that sometimes the telescope movements stop for a period of time.

When the off-axis guider is switched on the linear trend cannot be estimated in this way because the off-axis guider turns on the telescope motor to return the star to the guiding window. The linear trend in the Y-direction is not as strong as in the X-direction; nevertheless it also affects the telescope PSF.

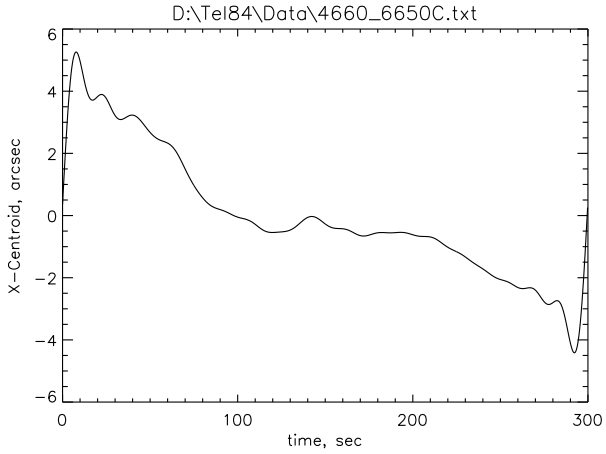

Fig. 2. A typical example of telescope linear long-term trend along the guiding direction (X-axis) cleaned from the high frequency components (see text for explanation of the signal filtering).

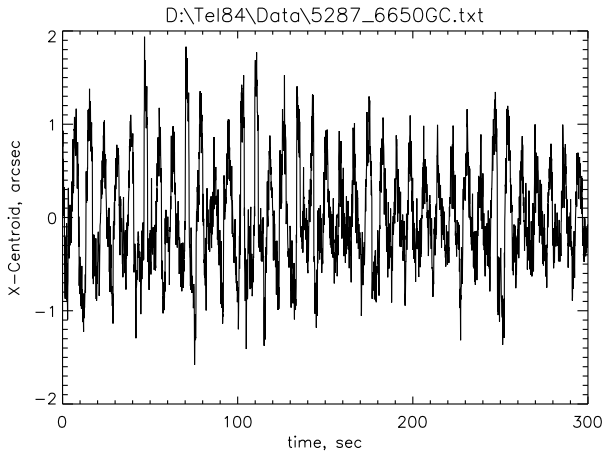

Fig. 3. Telescope oscillations along the guiding direction (X-axis).

4.2. *Telescope oscillations*

Another strong source of image distortions are the vibrations of the telescope. Figure 3 presents an example of the image centroid oscillation along the guiding direction (X-axis). This is a high frequency oscillation with a variable amplitude around ∼1.8 arcsec that in some cases can be overlayed by the linear trend as shown in Figure 1. Oscillations along the Y-axis have a lower amplitude (∼0.5 arcsec) than oscillations along the guiding X-axis and they are less relevant for widening the PSF in that direction.

Figure 4 presents the power spectra of the telescope oscillations obtained from the displacement of the image centroid. Analyzing the X-axis power

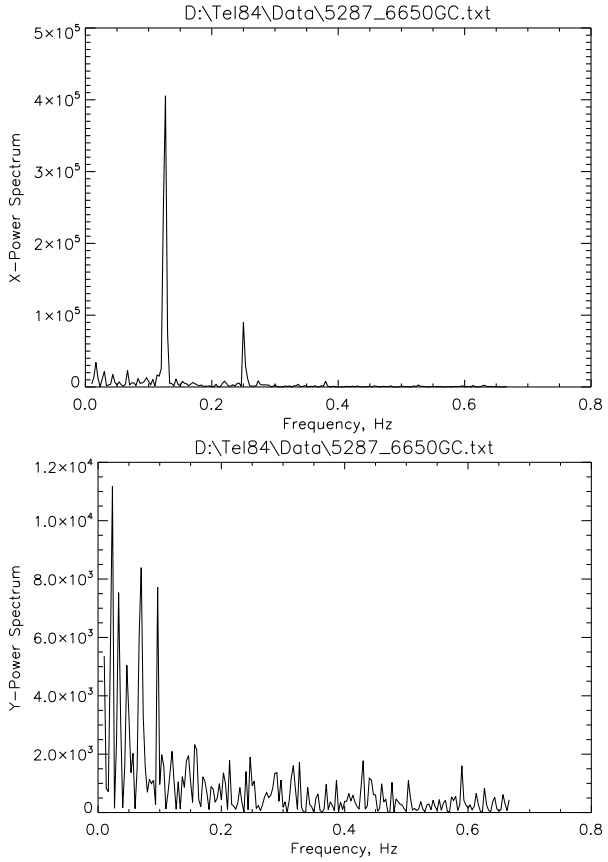

Fig. 4. Power spectra for the telescope oscillations. Upper panel: guiding direction (X-axis). Lower panel: declination (Y-axis).

spectrum in Figure 4 (upper graph), one can see two narrow peaks located at the frequencies 0.127 ± 0.008 and 0.254 ± 0.008 Hz (first harmonic). These frequencies are present in all our data.

In the Y-axis, the power spectrum of the centroid displacement shows several narrow peaks at frequencies lower than 0.1 Hz, as plotted in Figure 4. However, they are weaker than the ones in the X-axis and it seems that they are not permanent. In other words, the oscillations in the Y-direction are not as relevant as the ones in the X-direction.

4.3. *Telescope Jumps*

The third kind of guiding error that we noticed during our observations were telescope jumps. These jumps appear as fast image movements with a magnitude larger than 10 arcsec. They appear only in the Y-direction, with strong winds (more than 20 km/h), and in certain positions of the telescope. The occurrence of the jumps is quite rare. We noticed it visually only a few times during the two nights of observations. However, telescope jumps have a strong influence on stellar photometry. Figure 5 shows how the light flux is changing during the jump. One can see that the jump at the beginning is so big that the star disappears from the field of view. Then the star comes back, but after some time it disappears again.

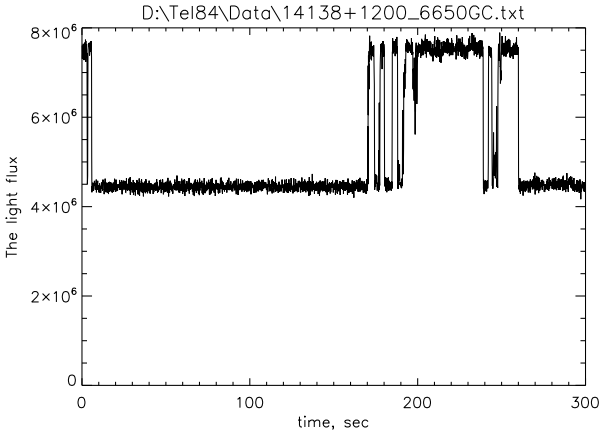

Fig. 5. Light flux variations during jumps of the telescope. Light flux is in arbitrary units. Object flux decreases due to several jumps of the telescope in the Y-direction (see text for explanation).

5. QUANTITATIVE RESULTS

In the previous section we have presented examples of the guiding errors found at the 0.84-m telescope and a qualitative analysis of each of them. Here we present a quantitative analysis of image degradation caused by the linear trends and oscillations on the telescope.

The motion of the centroid of the star image (Figure 1) can be separated in two parts: slow (Figure 2) and fast (Figure 3) motions. The standard deviations of these two parts are good quantitative parameters to evaluate them.

Table 1 presents the values of the standard deviations calculated for all series of observations. The first column contains the HD number of the observed star and the second column shows its declination. The third column gives the apparent visual magnitude of the star. The fourth column shows if the off-axis guider was switched on or off. The three following columns contain the measured standard deviations of the centroid motion along guiding direction where $\sigma 1_X$ is the standard deviation of the centroid motion, $\sigma 2_X$ is the standard deviation of the linear trend, and $\sigma 3_X$ is the standard deviation of the high-frequency centroid motion. The last three columns ($\sigma 1_Y$, $\sigma 2_Y$, and $\sigma 3_Y$) show the standard deviations

TABLE 1

STANDARD DEVIATIONS OF CENTROID MOTIONS

Name	Dec	Mag	Guider	$\sigma 1_X$	$\sigma 2_X$	$\sigma 3_X$	$\sigma 1_Y$	$\sigma 2_Y$	$\sigma 3_Y$
	(°)	V			(″)			(″)	
HD 122510	−31	6.18	Off	0.72	0.68	0.23	0.20	0.14	0.14
HD 122510	−31	6.18	On	0.28	0.10	0.26	0.19	0.12	0.14
HD 123123	−26	3.26	Off	1.23	1.11	0.51	0.52	0.45	0.25
HD 123123	−26	3.26	On	0.72	0.46	0.56	0.27	0.16	0.21
HD 114432	−24	7.90	Off	0.24	0.22	0.08	0.07	0.03	0.07
HD 114432	−24	7.90	On	0.11	0.08	0.08	0.10	0.08	0.07
HD 130412	−17	8.20	Off	0.63	0.61	0.14	0.11	0.07	0.09
HD 130412	−17	8.20	On	0.20	0.10	0.17	0.14	0.10	0.10
HD 108799	−13	6.35	Off	0.48	0.44	0.19	0.21	0.12	0.17
HD 108799	−13	6.35	On	0.40	0.19	0.35	0.50	0.20	0.45
HD 124517	+11	6.71	Off	0.85	0.80	0.27	0.19	0.11	0.16
HD 124517	+11	6.71	On	0.67	0.55	0.38	0.54	0.38	0.38
HD 157606	+13	7.48	Off	0.46	0.44	0.13	0.08	0.03	0.07
HD 157606	+13	7.48	On	0.20	0.04	0.20	0.11	0.05	0.09
HD 140232	+18	5.80	Off	1.11	1.08	0.25	0.22	0.16	0.15
HD 140232	+18	5.80	On	0.44	0.20	0.38	0.51	0.25	0.44
HD 130948	+23	5.88	Off	1.90	1.87	0.34	0.28	0.17	0.22
HD 130948	+23	5.88	On	0.34	0.09	0.32	0.27	0.17	0.20
HD 127665	+30	3.58	Off	2.95	2.90	0.54	0.44	0.40	0.18
HD 127665	+30	3.58	On	0.58	0.36	0.45	0.43	0.40	0.17
HD 145328	+36	4.76	Off	1.50	1.43	0.41	0.46	0.44	0.15
HD 145328	+36	4.76	On	0.40	0.15	0.37	0.18	0.11	0.14
HD 127762	+38	3.00	Off	1.73	1.70	0.34	0.54	0.51	0.16
HD 127762	+38	3.00	On	0.52	0.27	0.44	0.39	0.32	0.21
HD 145873	+47	7.99	Off	0.22	0.21	0.08	0.06	0.04	0.05
HD 145873	+47	7.99	On	0.07	0.04	0.06	0.06	0.02	0.05
HD 102224	+47	3.71	Off	2.75	2.71	0.49	0.21	0.18	0.12
HD 102224	+47	3.71	On	0.88	0.81	0.35	0.23	0.18	0.14
HD 154905	+54	5.69	Off	0.90	0.87	0.22	0.26	0.22	0.12
HD 154905	+54	5.69	On	0.29	0.19	0.22	0.30	0.27	0.12
HD 106591	+57	3.32	Off	2.14	2.06	0.53	0.37	0.33	0.17
HD 106591	+57	3.32	On	0.93	0.87	0.31	0.49	0.46	0.17
HD 109387	+69	3.88	Off	1.41	1.39	0.26	0.29	0.23	0.17
HD 109387	+69	3.88	On	0.26	0.15	0.22	0.63	0.52	0.31

of the centroid motion along the declination direction for each of the three previous cases.

6. CONCLUSIONS

1. The guiding system of the 0.84-m telescope has been analyzed through the movements of the star image centroid in a set of short-exposures images for different positions of the telescope.

2. It was found that, during some periods of time, the telescope just stops tracking for approximately 1 minute. This produces a linear trend of the image. The off-axis guider is able to correct partially for this effect. However, the correction of the linear trend increases the amplitude of the oscillations.

3. The telescope constantly oscillates at the frequency of 0.127±0.008 Hz along the guiding direction. The minimum amplitude of these oscillations is 0.2 arcsec; however, sometimes it is greater than 2 arcsec.

4. The off-axis guider works well. For example, when the off-axis guider is on, the averaged degradation of images due to guiding errors is 0.52 arcsec which is comparable to the distortions introduced by the atmospheric turbulence. However without the off-axis guider this value is larger by 2.5 times. Nevertheless, after the correction, the PSF still may have an asymmetrical shape. Unfortunately, the off-axis guider cannot correct telescope jumps due to their big amplitude and velocity. These jumps occur rarely, but they can very strongly affect the results of photometric observations.

5. We did not notice any dependence of guiding errors on the inclination of the telescope. The image quality can be improved by canceling the the telescope oscillations using some modern tip-tilt corrector.

We acknowledge the support from DGAPA-PAPIIT-Universidad Nacional Autónoma de México, grants IN104910 and IN112710.

REFERENCES

Altarac, S., Berlioz-Arthaud, P., Thiébaut, E., Foy, R., Balega, Y. Y., Dainty, J. C., & Fuensalida, J. J. 2001, MNRAS, 322, 141
Echevarría, J., et al. 1998, RevMexAA, 34, 47
Michel, R., Echevarría, J., Costero, R., Harris, O., Magallón, J., & Escalante, K. 2003, RevMexAA, 39, 291
Schöck, M., et al. 2009, PASP, 121, 384
Tapia, M. 2003, RexMexAA (SC), 19, 75
Tokovinin, A., & Cantarutti, R. 2008, PASP, 120, 170
Valdez, J., et al. 1997, Comisión Técnica Observatorio 97-1, Instituto de Astronomía, Universidad Nacional Autónoma de México, Mexico
Voitsekhovich, V. V., Orlov, V. G., Sánchez, L. J., & Garfias, F. 2007, RevMexAA, 43, 309
Zazueta, S. 1995, Reporte Técnico RT 95-04, Instituto de Astronomía, Universidad Nacional Autónoma de México, Mexico

V. G. Orlov and V. V. Voitsekhovich: Instituto de Astronomía, Universidad Nacional Autónoma de México, Apdo. Postal 70-264, C.P. 04510, México D.F., Mexico (orlov, voisteko@astro.unam.mx)
D. Hiriart: Instituto de Astronomía, Universidad Nacional Autónoma de México, Apdo. Postal 870, 2800 Ensenada, B.C., Mexico (hiriart@astrosen.unam.mx).